Sucrose Signaling Contributes to the Maintenance of Vascular Cambium by Inhibiting Cell Differentiation

Aoi Narutaki[1], Prihardi Kahar[2], Shunji Shimadzu[1,3], Shota Maeda[1], Tomoyuki Furuya[1,4], Kimitsune Ishizaki[1], Hidehiro Fukaki[1], Chiaki Ogino[2] and Yuki Kondo[1,*]

[1]Department of Biology, Graduate School of Science, Kobe University, 1-1 Rokkodai, Kobe, 657-8501 Japan
[2]Department of Chemical and Engineering, Graduate School of Engineering, Kobe University, 1-1 Rokkodai, Kobe 657-8501, Japan
[3]Department of Biological Sciences, Graduate School of Science, The University of Tokyo, 7-3-1 Hongo, Bunkyo-ku, Tokyo 113-0033, Japan
[4]College of Life Sciences, Ritsumeikan University, 1-1-1 Noji-higashi, Kusatsu 525-8577, Japan

*Corresponding author: E-mail, pkondo@tiger.kobe-u.ac.jp

Plants produce sugars by photosynthesis and use them for growth and development. Sugars are transported from source-to-sink organs via the phloem in the vasculature. It is well known that vascular development is precisely controlled by plant hormones and peptide hormones. However, the role of sugars in the regulation of vascular development is poorly understood. In this study, we examined the effects of sugars on vascular cell differentiation using a vascular cell induction system named 'Vascular Cell Induction Culture System Using Arabidopsis Leaves' (VISUAL). We found that sucrose has the strongest inhibitory effect on xylem differentiation, among several types of sugars. Transcriptome analysis revealed that sucrose suppresses xylem and phloem differentiation in cambial cells. Physiological and genetic analyses suggested that sucrose might function through the BRI1-EMS-SUPPRESSOR1 transcription factor, which is the central regulator of vascular cell differentiation. Conditional overexpression of cytosolic invertase led to a decrease in the number of cambium layers due to an imbalance between cell division and differentiation. Taken together, our results suggest that sucrose potentially acts as a signal that integrates environmental conditions with the developmental program.

Keywords: Stem cell ● Sucrose ● Sugar signaling ● Vasculature ● VISUAL

Introduction

Plants undergo carbon assimilation via photosynthesis to produce sugars. During the day, sugars are stored as starch, whereas at night, they are degraded to buffer sugar contents, enabling continuous sugar supply for growth. Sugars are used as energy sources and cell wall materials in plants. Under fluctuating environmental circumstances, plants need to sense their sugar status to maximize growth and development according to photosynthetic productivity. So far, numerous studies have proposed important functions of sugars as developmental signals. For example, hexokinases (HXKs), which catalyze the phosphorylation of glucose in the glycolytic pathway, also function as sugar sensors to regulate growth and development (Moore et al. 2003, Li and Sheen 2016). Another key protein in a sugar-triggered signaling is TARGET OF RAMAMYCIN (TOR), which commonly shares this function in eukaryotes. *TOR* encodes a protein kinase that forms a complex with Regulatory-Associated Protein of TOR and small lethal with SEC13 protein 8 to phosphorylate diverse substrates upon energy sensing (Shi et al. 2018). TOR is activated by glucose to phosphorylate ETHYLENE INSENSITIVE 2, a key regulator in ethylene signaling, thereby promoting cell division in the root meristem (Fu et al. 2021). Moreover, recent studies have shown that TOR interacts with a component of POLYCOMB REPRESSIVE COMPLEX2 to change the histone modification H3K27me3 globally in the genome (Dong et al. 2023, Ye et al. 2022).

Sugars take various forms in plants, and most of them are categorized as reducing sugars. As a non-reducing sugar, sucrose is stably transported throughout the plant body from source-to-sink organs via the vascular phloem tissue (Lemoine et al. 2013). Vascular cells consisting of several cell types are commonly generated from stem cells located in the cambium meristem (Shi et al. 2017). At present, it is widely recognized that plant hormones and peptides play pivotal roles in the regulation of secondary vascular development (Fukuda and Hardtke 2020). As a peptide hormone, tracheary element differentiation inhibitory factor (TDIF) is recognized by its receptor TDIF RECEPTOR/PHLOEM INTERCALATED WITH XYLEM (TDR)/(PXY) in the cambium (Ito et al. 2006, Fisher and Turner 2007, Hirakawa et al. 2008, 2010, Etchells and Turner 2010, Kondo et al. 2014). Upon TDIF perception, TDR activates GLYCOGEN SYNTHASE KINASE 3s (GSK3s) and then represses the activity of the BRI1-EMS-SUPPRESSOR1 (BES1) transcription factor to regulate vascular stem cell maintenance (Kondo et al. 2014, Saito et al. 2018, Furuya et al. 2021). Furthermore, numerous studies have identified additional regulators that function together with TDIF–TDR signaling, thus forming

complex regulatory networks (Kondo and Fukuda 2015, Etchells et al. 2016, Shimadzu et al. 2023). In addition to such developmental programs, cambium activity is affected by seasonal factors, as observed in the annual rings of tree species. However, little is known about how environmental cues control vascular development.

Recent studies have provided evidence for the involvement of sugars in vascular development. Transcriptome reanalysis revealed that several key regulators of vascular development, including *CLAVATA3/EMBRYO SURROUNDING REGION-related 41* that encodes TDIF, are affected by glucose and sucrose at the transcript level (Dinant and Le Hir 2022). In addition, antisense suppression of the gene encoding fructokinase (FRK2) in tomatoes caused abnormalities in xylem and phloem development (Damari-Weissler et al. 2009, Lugassi et al. 2022). However, the direct effects of sugars on vascular development have not been well studied, because the vasculature is very deeply located. A tissue culture system Vascular Cell Induction Culture System Using Arabidopsis Leaves (VISUAL) has been used to investigate the impact of signaling molecules in the regulation of vascular development from physiological and genetic approaches (Kondo et al. 2015, 2016). Here, we show that sucrose treatment inhibits xylem and phloem differentiation from cambial cells using VISUAL. This inhibitory effect of sucrose was not observed in the dominant *bes1-D* mutant. Furthermore, overexpression of a gene encoding a cytosolic invertase, which catalyzes the hydrolysis of sucrose into glucose and fructose, canceled the sucrose effects in VISUAL and decreased cambium layers in the hypocotyl vasculature.

Results

The effects of sugars on xylem differentiation in VISUAL

The VISUAL culture medium contains 5% (w/v) glucose. To test the effects of sugars on xylem differentiation in VISUAL, transgenic *Arabidopsis* harboring a xylem-specific luminescent marker, in which Emerald luciferase (ELUC) was driven by the promoter of *IRREGULAR XYLEM 3* (*IRX3*), were used (Kondo 2022). *pIRX3:ELUC* seedlings were cultured in the VISUAL medium containing several kinds of sugars instead of glucose (Fig. 1A). For auto-measurement, *pIRX3:ELUC* cotyledons were subjected to VISUAL containing the LUC substrate luciferin, and luminescence was recorded using a luminometer according to a method described previously (Tamaki et al. 2020). Conventional VISUAL medium containing glucose significantly increased the luminescence of *pIRX3:ELUC* due to ectopic induction of xylem differentiation (Fig. 1B). Similar results were obtained when the monosaccharide galactose and the disaccharide maltose were used at 5% (w/v) (Fig. 1B). However, the monosaccharide fructose and the disaccharide sucrose induced only relatively weak luminescence (Fig. 1B). Quantification of the integrating values of LUC luminescence revealed that xylem differentiation is not significantly induced in the samples treated with fructose or sucrose, compared to other types of sugars (Fig. 1C). Next, we examined ectopic xylem differentiation in VISUAL and quantified its area per whole leaf area. Among the tested sugars, sucrose had the strongest inhibitory effect on the xylem differentiation area (Fig. 1D, E), which was consistent with the results of the LUC assay (Fig. 1B, C). Hereafter, we will focus sucrose as a sugar that potentially regulates vascular development.

Sucrose inhibits xylem differentiation in VISUAL in a dose-dependent manner

To test the impact of sucrose, we changed the ratio of glucose and sucrose in the VISUAL medium and then conducted a quantitative xylem cell fate assay using the xylem luminescent marker *pIRX3:ELUC*. As the sucrose ratio increased, *pIRX3:ELUC* luminescence gradually decreased (Fig. 2A, B). Next, we changed the concentration of sucrose when the glucose concentration was set to 2.5% (w/v). As the sucrose concentration increased, luminescence gradually decreased (Fig. 2C, D), suggesting that sucrose concentration is important for the inhibition of xylem differentiation. However, in this VISUAL assay, the osmotic pressure of the induction medium varies depending on the type of sugar: glucose (monosaccharide) or sucrose (disaccharide). To examine the effect of osmotic pressure on xylem differentiation in VISUAL, we measured *pIRX3:ELUC* luminescence at similar molar concentrations of glucose and sucrose. Sucrose induced much fewer ectopic xylem cells than glucose regardless of molar concentration (Supplementary Fig. S1). Taken together, these results suggest that sucrose treatment inhibits xylem differentiation in a dose-dependent manner.

Sucrose inhibits xylem and phloem differentiation to accumulate cambial cells

Next, the effects of sucrose on vascular-related gene expression were examined using microarray and RNA-seq analysis (Fig. 3A). Previously, we identified cambium-, xylem- and phloem-related genes by co-expression network analysis with the time-course and tissue-specific VISUAL transcriptome datasets (Furuya et al. 2021). RNA-seq analysis using cotyledon samples cultured in VISUAL for 72 h revealed that sucrose increases the expression of cambium-related genes more than glucose (Fig. 3B). By contrast, the expression of xylem- and phloem-related genes was lower in samples treated with sucrose than glucose, suggesting that sucrose inhibits cell differentiation from the cambium to xylem or phloem (Fig. 3B). Similarly, we conducted microarray experiments using leaf-disk samples cultured in VISUAL for 0, 24 and 48 h. In this leaf-disk VISUAL assay (Kondo et al. 2015), sucrose weakly induced the expression of xylem- and phloem-related genes and resulted in the accumulation of cambium-related transcripts 48 h after induction (Fig. 3C). Phloem sieve element differentiation can be visualized with the phloem-fluorescent marker *gRABC2A-GFP* (Nurani et al. 2020). Compared to VISUAL with glucose, VISUAL with sucrose was less effective in inducing the ectopic formation of phloem sieve elements as well as xylem cells (Fig. 3D).
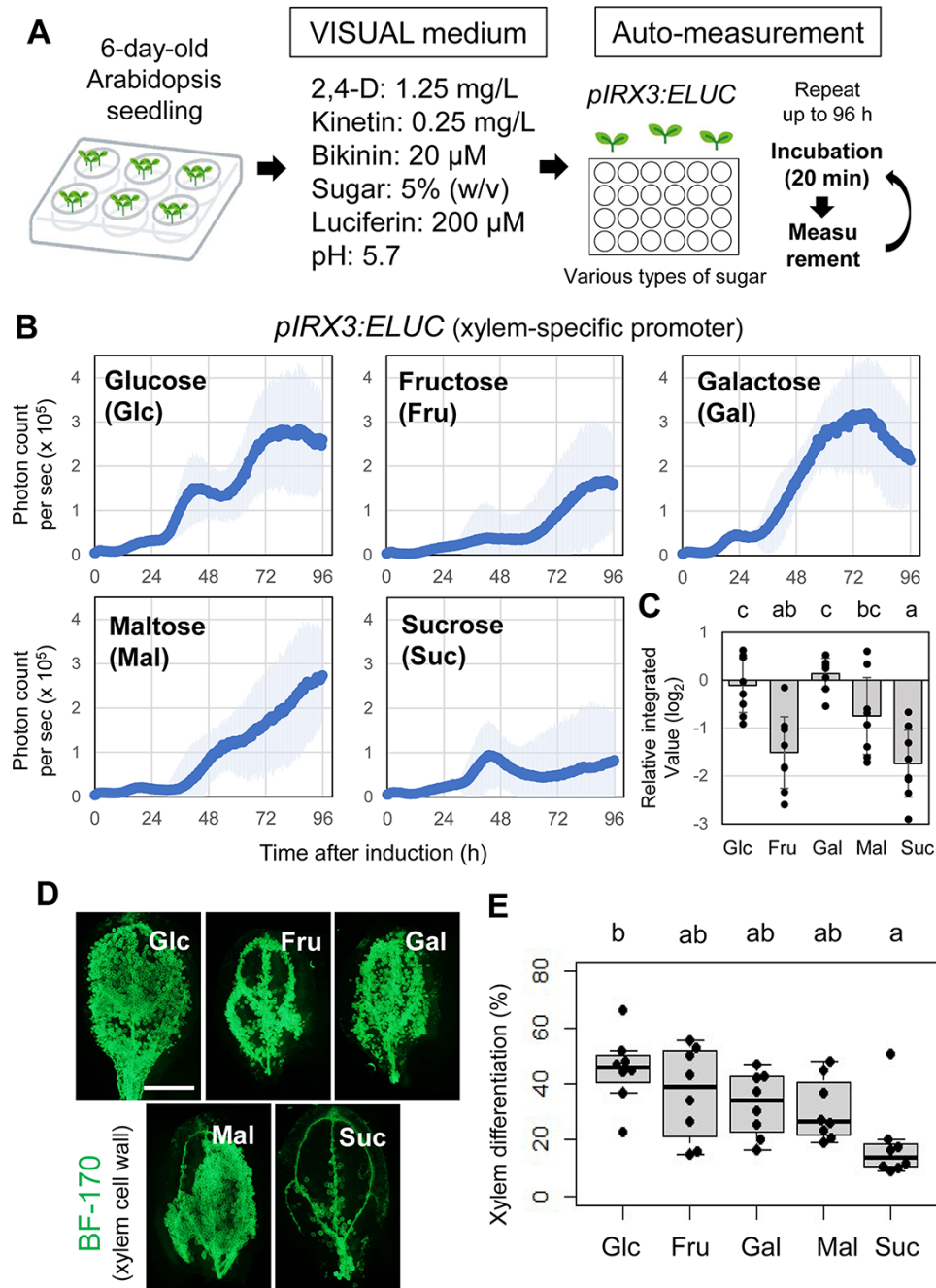
Fig. 1 The effects of different types of sugars on xylem differentiation in VISUAL. (A) The experimental procedure for the time-course quantification of the luminescence of xylem marker *pIRX3:ELUC* in VISUAL using a luminometer. (B) The effects of several types of sugars at 5% (w/v) on the luminescence of *pIRX3:ELUC* in VISUAL ($n = 8$). Data are mean ± standard deviation. (C) The integrated value of luminescence was calculated from the graph in (B). The relative score was calculated when the mean value of Glc was set to 1 and is shown in the $\log_2$ scale. Statistical differences are indicated with different letters ($n = 8$; Tukey–Kramer test). Error bars indicate standard deviation. (D) Ectopic xylem differentiation induced by several types of sugars in VISUAL was visualized using the secondary cell wall fluorescent indicator BF-170. Scale bar: 1 mm. (E) Box-and-whisker plots of the xylem differentiation rate (%) calculated from the images in (D). Statistical differences are indicated with different letters ($n = 8$; Tukey–Kramer test).

The relationship between BES1 and sucrose signaling

The effects of sucrose resembled the phenotype of the *bes1* loss-of-function mutant, which also shows the inhibition of xylem and phloem differentiation that leads to the accumulation of cambial cells in VISUAL (Saito et al. 2018). We compared the time courses of the transcriptome profiles of wild type (WT) (0–72 h; Furuya et al. 2021), *bes1-1* (72 h; Saito et al. 2018),
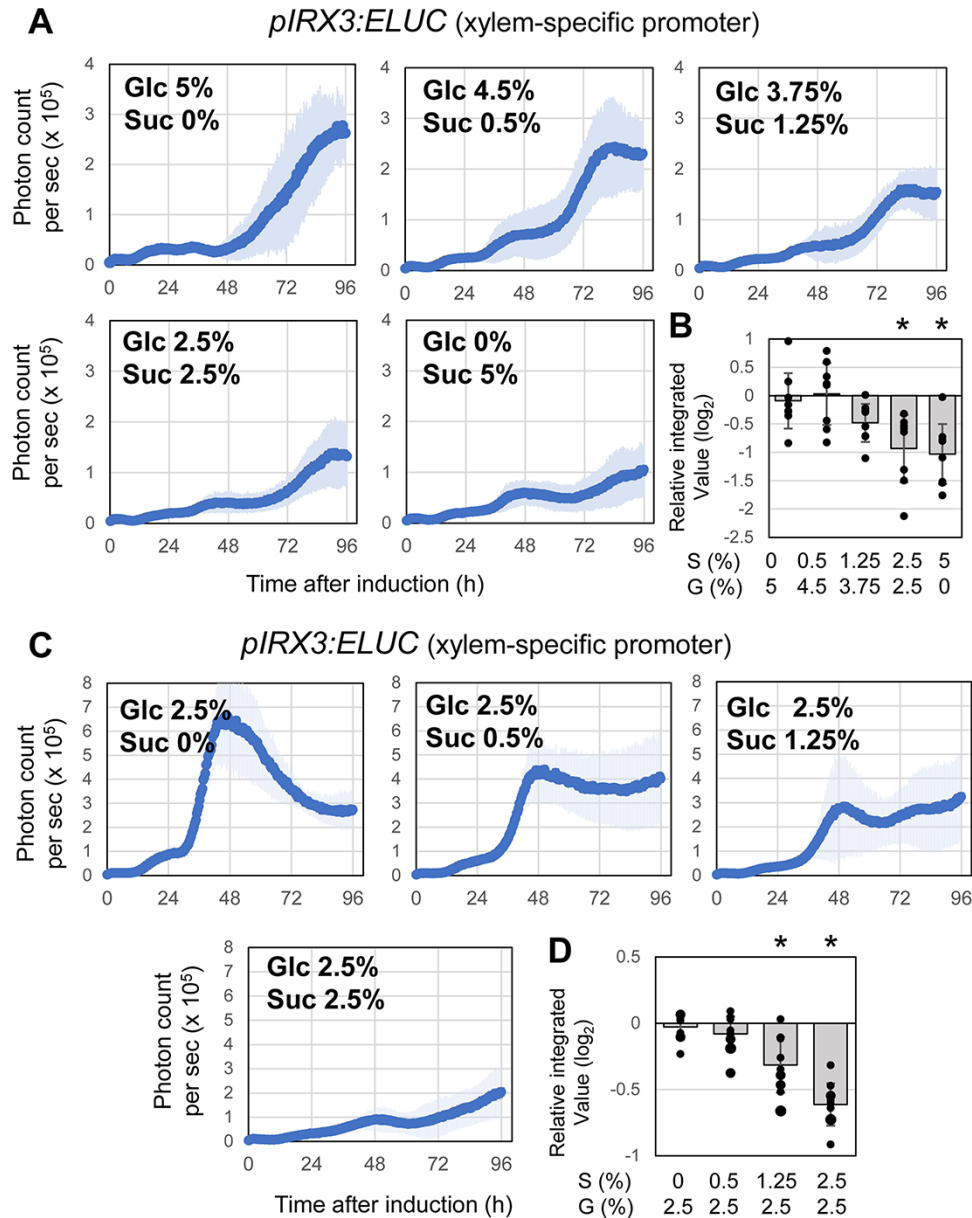
Fig. 2 The combinatory effects of glucose and sucrose on xylem differentiation in VISUAL. (A) The effects of glucose (Glc) and sucrose (Suc) on the luminescence of *pIRX3:ELUC* in VISUAL (*n* = 8), when the ratio of Glc to Suc was varied. Data are mean ± standard deviation. (B) The integrated value of luminescence was calculated from the graph in (A). The relative score was calculated when the mean value of Glc 5% and Suc 0% was set to 1 and is shown in the log$_2$ scale. Statistical differences are indicated with different letters (*n* = 8; Tukey–Kramer test). Error bars indicate standard deviation. (C) The dose-dependent effects of sucrose on the luminescence of *pIRX3:ELUC* in VISUAL (*n* = 9–10), when the Glc concentration was set to 2.5% (w/v). Data are mean ± standard deviation. (D) The integrated value of luminescence was calculated from the graph in (C). The relative score was calculated when the mean value of Glc 2.5% and Suc 0% was set to 1 and is shown in the log$_2$ scale. Statistical differences are indicated with different letters (*n* = 9–10; Tukey–Kramer test). Error bars indicate the standard deviation.

apl (72 h; Kondo et al. 2016), glucose (0, 24 and 48 h; this study) and sucrose (0, 24 and 48 h; this study). Principal component analysis (PCA) with a focus on VISUAL-induced genes (844 genes) revealed that the transcript profile of sucrose 48 h resembled that of *bes1-1* 72 h and that the transcript profile of glucose 48 h was similar to that of WT 72 h (**Fig. 4A**). Fold changes in gene expression, calculated from RNA-seq data,

between sucrose 72 h and glucose 72 h also strongly correlated with those calculated from microarray data between *bes1* 72 h and WT 72 h (**Fig. 4B**). These results suggest that sucrose inhibits xylem and phloem differentiation in a similar manner to the *bes1* loss-of-function mutant. To examine the relationship between sucrose and BES1, the gain-of-function mutant *bes1-D* was analyzed using VISUAL in the presence or absence
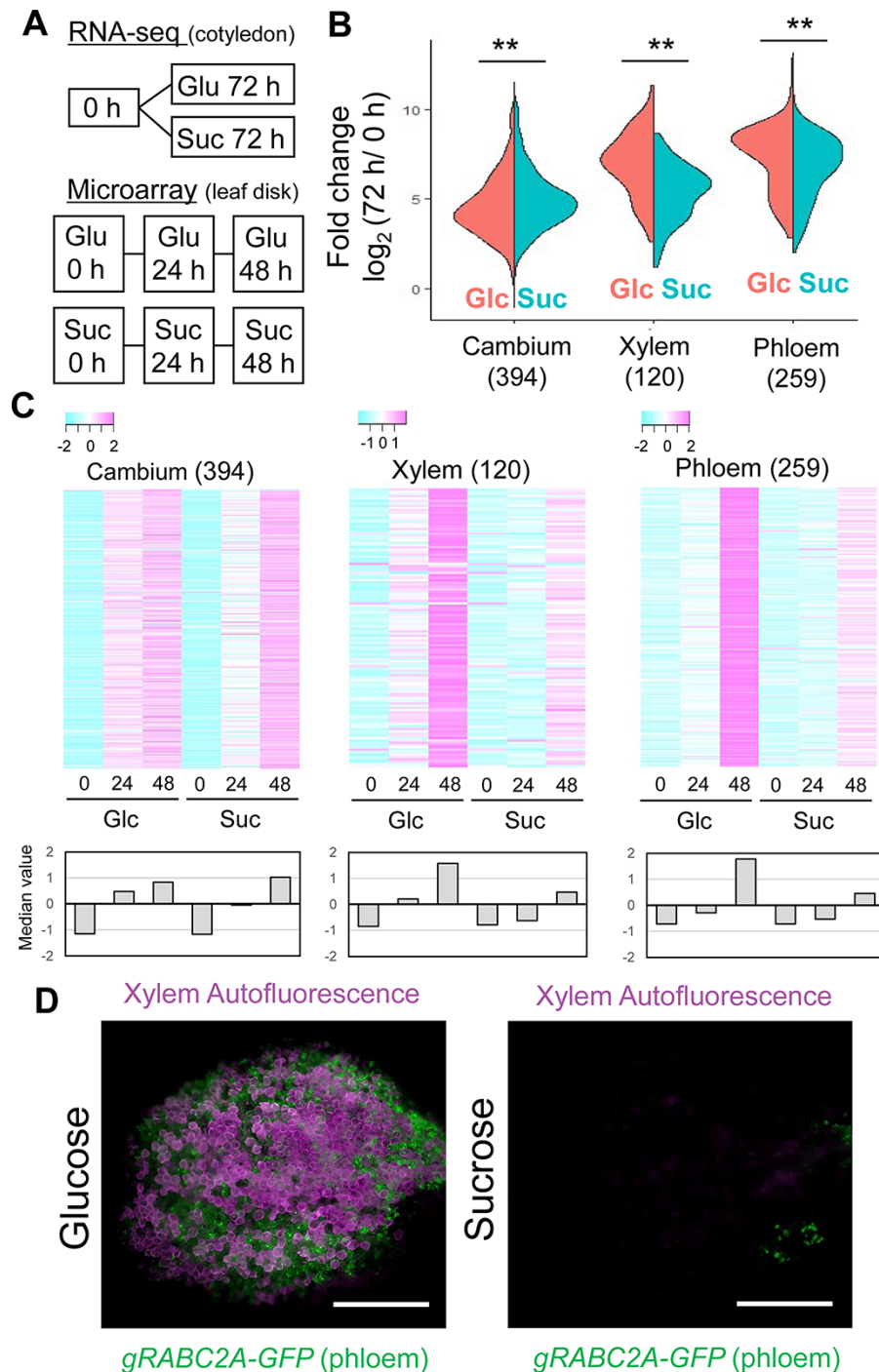
Fig. 3 The effects of sucrose on xylem and phloem differentiation in VISUAL. (A) A schematic of the design of RNA-seq and microarray analysis in glucose (5%) or sucrose (5%) VISUAL. (B) Fold changes ($\log_2$) in cambium-, xylem- and phloem-related gene expression in glucose or sucrose VISUAL RNA-seq data (72/0 h) are shown as a split violin plot. Statistical differences were analyzed using Student's *t*-test (**$P < 0.01$). (C) Heatmaps of *z*-scores for cambium-, xylem- and phloem-related gene expression in glucose or sucrose VISUAL microarray data (0, 24 and 48 h). Color scales are shown above the panels. Median values of *z*-scores are shown in the lower panels. (D) Phloem sieve element differentiation in glucose or sucrose VISUAL was visualized using the phloem marker *gRABC2A-GFP*. Scale bars: 1 mm.

of sucrose. The *bes1-D* mutants ectopically formed xylem cells at relatively low frequency, even in VISUAL with glucose (**Fig. 4C, D**), perhaps due to the narrow cotyledons resulting from the elevation of brassinosteroid (BR) signaling outputs. Nevertheless, the xylem differentiation rate of the *bes1-D* mutant in VISUAL with sucrose was similar to that of the
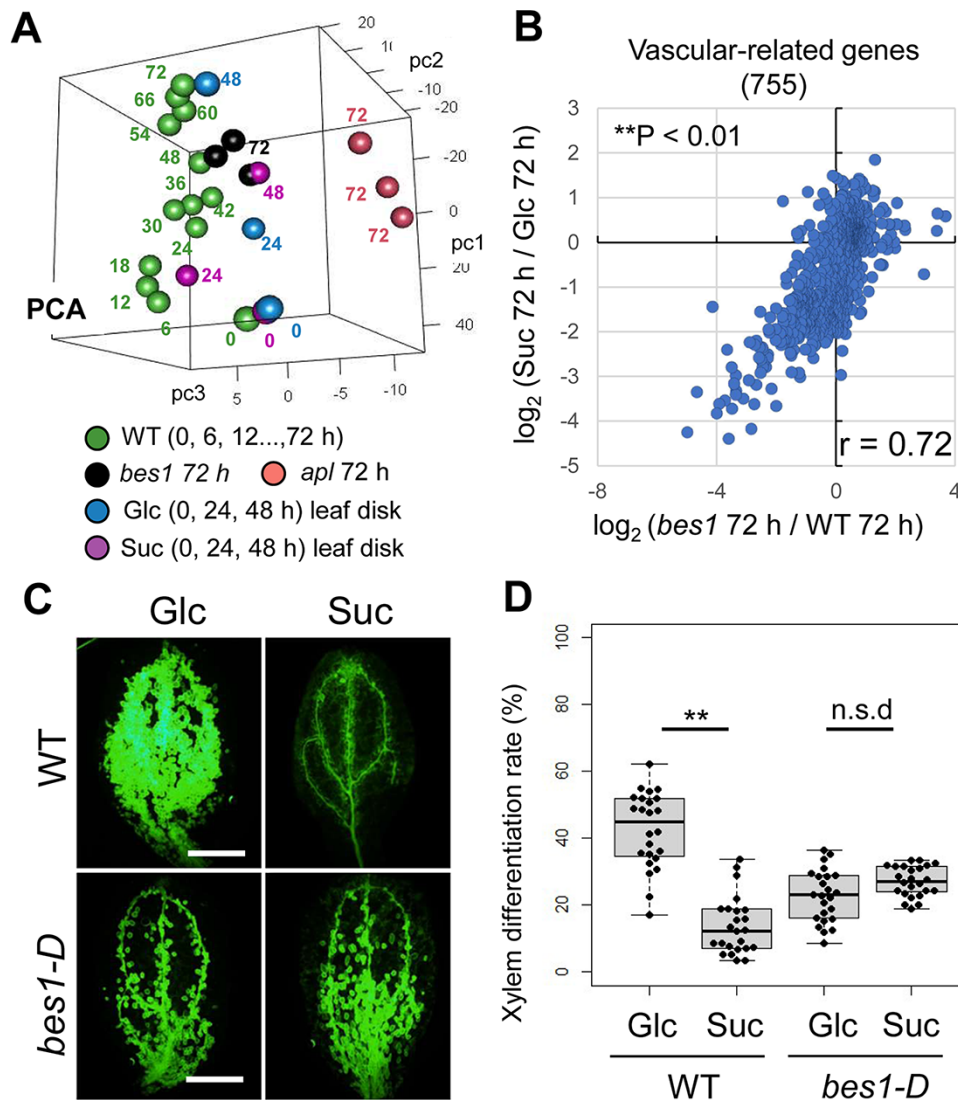
Fig. 4 The relationship between sucrose and BES1 in VISUAL. (A) PCA of VISUAL transcriptome data of WT time-course, *bes1* 72 h, *apl* 72 h, Glc 0 h, 24 h and 48 h and Suc 0 h, 24 h and 48 h is shown as a three-dimensional plot. (B) Correlation between the fold changes of Suc 72 h versus Glc 72 h and those of *bes1* 72 h versus WT 72 h. Dot plots indicate vascular-related genes and significant differences (Pearson correlation coefficient, **$P < 0.01$). (C) Ectopic xylem differentiation induced by glucose or sucrose in VISUAL was visualized using the secondary cell wall fluorescent indicator BF-170. Scale bars: 1 mm. (D) Box-and-whisker plots of the xylem differentiation rate (%) calculated from the images in (C). Statistical differences were analyzed using Student's *t*-test in each genotype ($n = 24$; **$P < 0.01$; n.s.d., no significant difference).

bes1-D mutant in VISUAL with glucose (**Fig. 4C, D**). These results suggest that sucrose might inhibit xylem differentiation through inactivating the BES1 transcription factor.

As a central regulator of sugar signaling, the TOR pathway is well known to control growth and development. To test the involvement of TOR in the sucrose-dependent suppression of xylem differentiation, we used a TOR inhibitor, AZD-8055, in the VISUAL assay (Chresta et al. 2010). AZD-8055 treatment at 0.5 and 1.0 μM, which does not cause severe defects in leaf development (Dong et al. 2015), did not erase the inhibitory effect of sucrose on xylem differentiation (**Supplementary Fig. S2**). However, AZD-8055 unexpectedly attenuated xylem differentiation in VISUAL with glucose (**Supplementary Fig. S2**),

suggesting that glucose might promote xylem differentiation, probably through TOR.

Overproduction of cytosolic invertase diminishes cambium activity in plants

CYTOSOLIC INVERTASE 1 (*CINV1*) encodes a cytosolic invertase, which irreversibly and specifically digests sucrose into glucose and fructose at neutral pH (Lou et al. 2007, Xiang et al. 2011). We investigated the vascular phenotype of a *CINV1* conditional overexpression line (*pER8:CINV1-CFP*). reverse transcription quantitative real-time PCR (RT-qPCR) experiments confirmed that *CINV1* expression is significantly induced
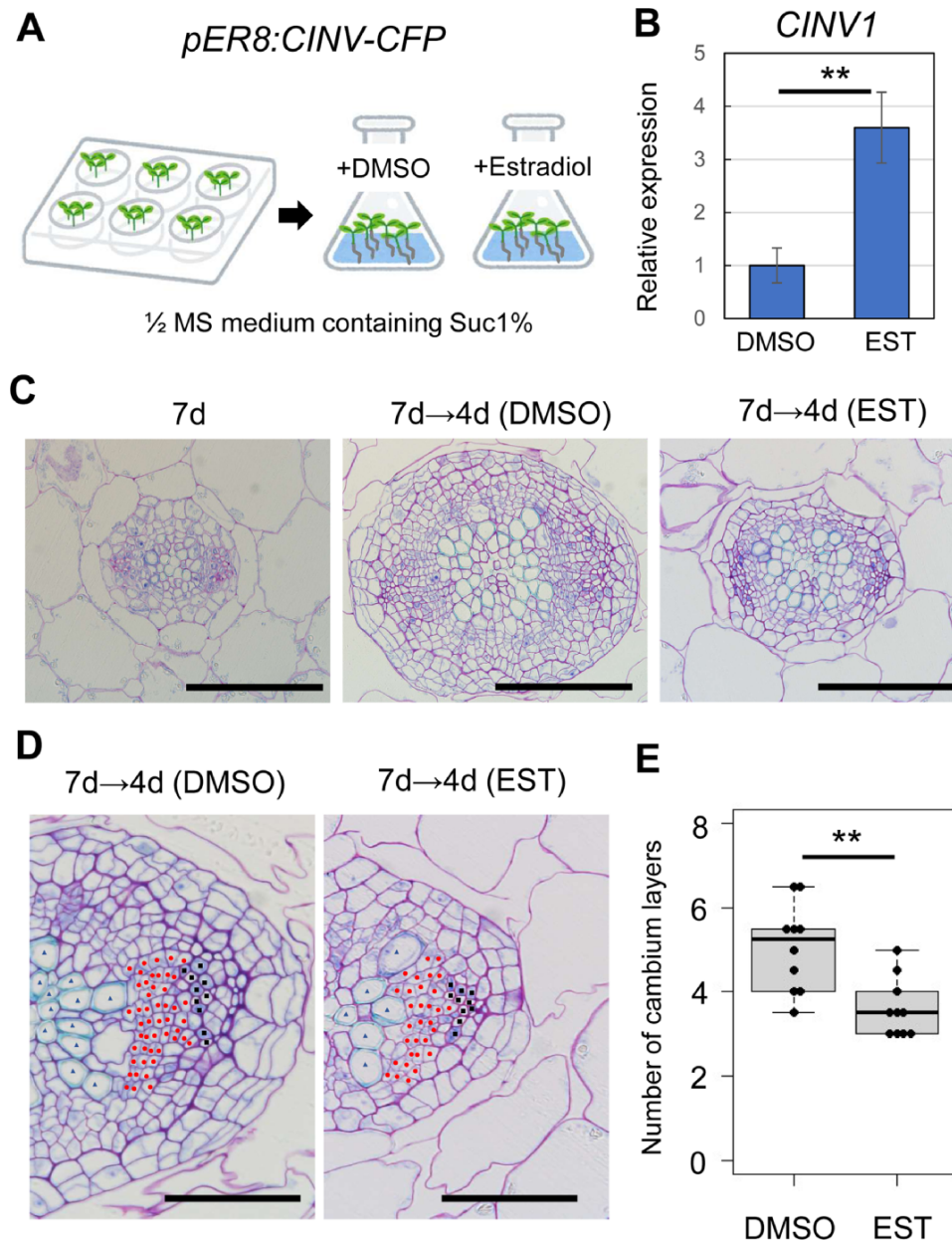
Fig. 5 The effects of CINV1 overproduction on the development of hypocotyl vasculature. (A) The experimental design of inducing *CINV1* overexpression for phenotypic analysis in the hypocotyl vasculature. (B) Relative expression levels of *CINV1* in *pER8:CINV1-CFP* plants treated with DMSO or EST were normalized with the expression levels of an internal control gene (*UBQ14*) ($n = 3$). (C) Transverse sections of 11-day-old *pER8:CINV1-CFP* seedlings treated with DMSO or EST according to the method described in (A). (D) Higher magnification images of (C). Xylem vessels, cambial cells and phloem cells are indicated by dots on the section. (E) Calculation of the minimum number of cambium layers from cross-sectional images. The number of cambium layers is shown with box-and-whisker plots ($n = 10$). Statistical differences were analyzed using Student's *t*-test (**$P < 0.01$). Scale bars: 100 μm (C) and 500 μm (D).

upon estradiol treatment in transgenic plants (**Fig. 5A, B**). To investigate the function of *CINV1* overexpression in relation to the effect of sucrose, we conducted a VISUAL assay using *pER8:CINV1-CFP* transgenic plants. Estradiol-inducible overexpression had no impact on xylem differentiation in VISUAL with 5% glucose (**Fig. 6A, B**). DMSO-treated WT cotyledons

barely formed ectopic xylem cells in VISUAL with 2.5% glucose plus 2.5% sucrose (**Fig. 6**), whereas estradiol-inducible *CINV1* overexpression led to ectopic xylem formation under the same culture conditions (**Fig. 6C, D**). Consequently, CINV1 overproduction could suppress the inhibitory effect of sucrose on xylem differentiation. For the analysis of in vivo vascular
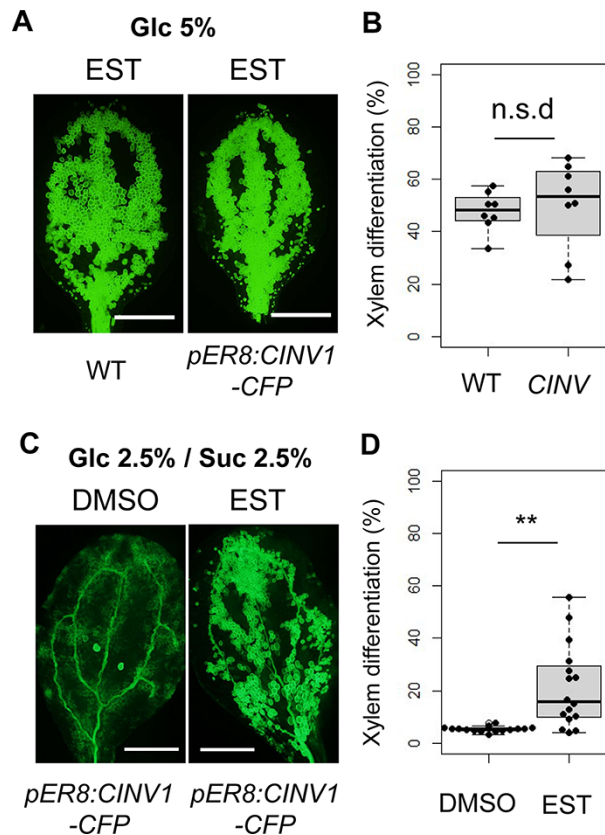
Fig. 6 The effects of CINV1 overproduction on xylem differentiation in VISUAL. (A) Ectopic xylem differentiation induced by Glc 5% VISUAL in WT and *pER8:CINV1-CFP* in the presence of 10 μM estradiol. (B) Box-and-whisker plots of the xylem differentiation ratio (%) calculated from the images in (A) ($n = 10$). (C) Ectopic xylem differentiation induced by Glc 2.5%/Suc 2.5% VISUAL in WT and *pER8:CINV1-CFP* in the presence of 10 μM estradiol. (D) Box-and-whisker plots of the xylem differentiation rate (%) calculated from the images in (C) ($n = 15–16$). Statistical differences were analyzed using Student's *t*-test (**$P < 0.01$; n.s.d., no significant difference). Scale bars: 1 mm.

development, 7-day-old *pER8:CINV1-CFP* seedlings were transferred to a medium containing DMSO or estradiol and incubated for 4 d (**Fig. 5A**). Estradiol-treated *CINV1* overexpression lines had smaller hypocotyl vasculature than DMSO-treated plants (**Fig. 5C**). Detailed phenotypic examination indicated that the number of cambium layers was reduced by *CINV1* overexpression (**Fig. 5D, E**). On the other hand, the numbers of xylem vessels, phloem sieve elements and companion cells were not significantly altered upon *CINV1* overexpression (**Supplementary Fig. S3**). Cambium layers are controlled by cell differentiation and cell proliferation in the cambium. These results suggest the possibility that the lack of sucrose has negative impacts on cambium maintenance by unbalancing cell differentiation and proliferation.

To investigate the role of sucrose in cambium regulation in more detail, gene set enrichment analysis (GSEA) was performed to statistically identify enriched Gene Ontology (GO) terms in the VISUAL transcriptome datasets (Subramanian et al. 2005). Consistent with the results showing that xylem differentiation was suppressed by sucrose, genes related to the secondary cell wall, which is preferentially developed in xylem cells, were enriched in sucrose-downregulated genes (**Fig. 7A, B**). By contrast, translation-related and cell

cycle–related terms were enriched in sucrose-upregulated genes (**Fig. 7A, B**). These results suggest that sucrose is involved in the developmental switch from cell differentiation to cell division in the cambium. Collectively, the results suggest that the sucrose signal maintains the cambium by inhibiting cell differentiation and indirectly or directly promoting cell proliferation (**Fig. 7C**).

Discussion

To date, numerous studies have demonstrated the importance of hormones and peptides in the regulation of vascular development. In this study, we demonstrated that sucrose inhibits xylem differentiation in a dose-dependent manner in VISUAL. Sucrose is a disaccharide composed of glucose and fructose. Xylem differentiation was partially suppressed in the presence of fructose (**Fig. 1**), raising the possibility that fructose produced by hydrolysis of sucrose inhibits xylem differentiation in the case of VISUAL with sucrose. However, *CINV1* overexpression diminished the inhibitory effect of sucrose on xylem differentiation (**Fig. 6**), suggesting that sucrose itself acts to inhibit xylem differentiation. When converted to molar concentrations, sucrose inhibited xylem differentiation
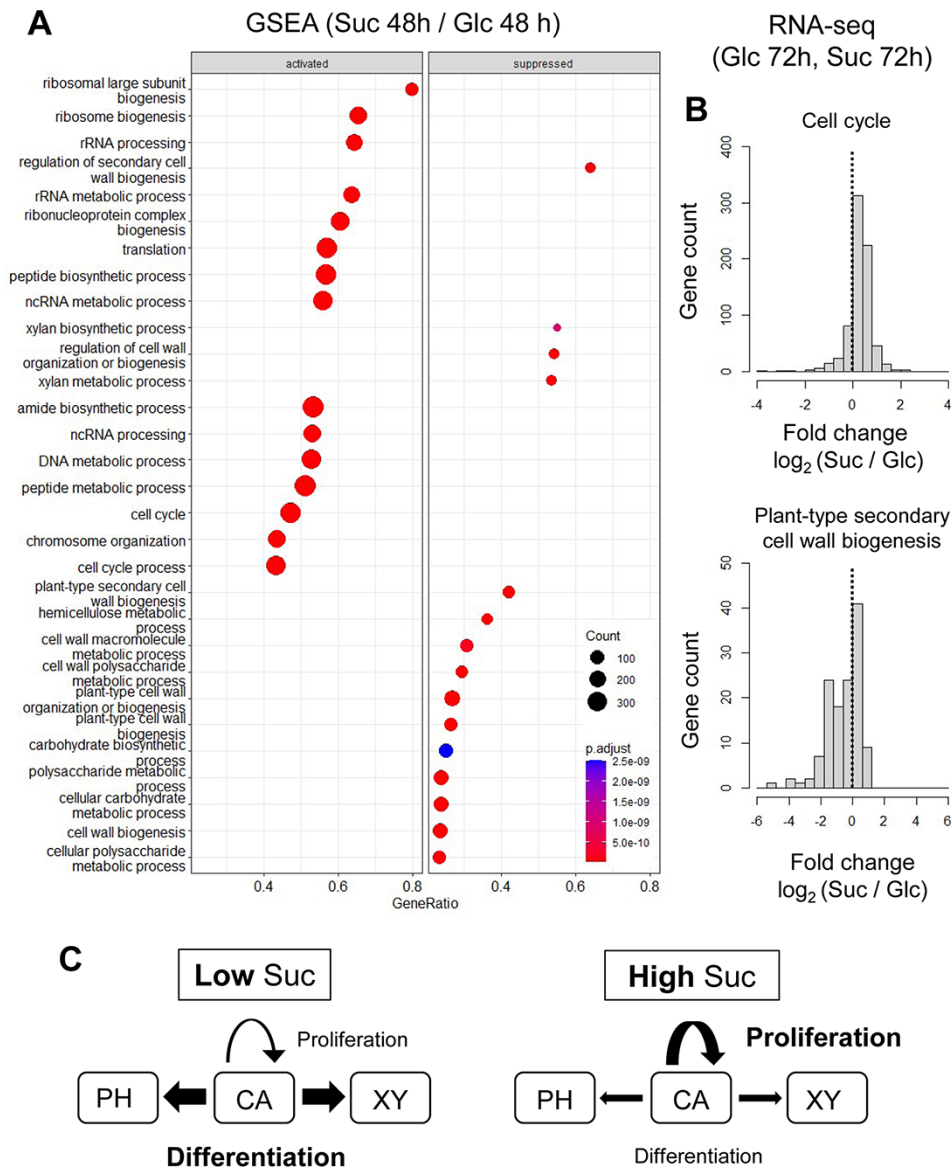
Fig. 7 Sucrose balances cell proliferation and differentiation in vascular development. (A) GSEA of glucose versus sucrose microarray datasets (48 h). Enriched GO terms (top 30) revealed by GSEA are shown as dot plots. (B) Fold changes ($\log_2$ of sucrose 72 h/glucose 72 h) for the GO terms 'cell cycle' and 'plant-type secondary cell wall biogenesis' shown as histograms. (C) Schematic illustration of the roles of sucrose in balancing cell proliferation and differentiation in the cambium.

at 38–75 mM in VISUAL (**Fig. 2D**). This range is similar to the sucrose concentration in the cytosol of mesophyll cells in tree species (Fink et al. 2018). Moreover, in the phloem sap of tree species, sucrose is present at a much higher concentration (∼800 mM) (Fink et al. 2018). In the vasculature of Scots pine, sucrose is degraded by Suc synthase (SuSy) in the phloem and the secondary wall forming xylem, resulting in concentration gradients from the phloem to cambium and xylem (Uggla et al. 2001). As another example, it was reported that sucrose leakage from the phloem tissue affects xylem development in *Arabidopsis* (Aubry et al. 2022). Sucrose concentrations in plants may reflect the status of sugar production by photosynthesis and sugar allocation from source-to-sink organs. Thus, our results

suggest that the proliferative activity of cells in the vascular cambium might be related to photosynthetic activity and sugar allocation affected by seasonal effects. Sensing of sucrose as a carbon resource could be an important adaptive mechanism for plants to integrate environmental information with growth and development.

As for the developmental program in the regulation of vascular development, TDIF–TDR–GSK3s–BES1 signaling competitively functions with BR–BRI1–GSK3s–BES1 to regulate xylem cell differentiation (Kondo et al. 2014, Kondo 2022). Furthermore, the competitive relationship among BES1 family members enables the robust regulation of vascular stem cells (Furuya et al. 2021). Recently, BES1 was also reported to function in

vascular cell proliferation by directly repressing *WOX4* expression (Hu et al. 2022). Aside from these fine-tuned mechanisms, transcriptome and genetic analyses revealed that sucrose influences vascular cell differentiation, most likely via BES1. Our previous studies have shown that *bes1-D* impairs cambium maintenance through excessive cell differentiation in plants (Kondo et al. 2014, Saito et al. 2018, Furuya et al. 2021). *CINV1* overexpressors have fewer cambium layers, which resemble the phenotype of the *bes1-D* mutant (Kondo et al. 2014, Furuya et al. 2021). Taken together, these studies suggest that sucrose positively regulates cambium maintenance by inhibiting cell differentiation and promoting cell proliferation through inactivating BES1. The *bes1-D* mutant has an amino acid substitution in the PEST sequence, which increases its protein stability (Yin et al. 2002). Understanding of the molecular mechanism governing the regulation of BES1 by sucrose requires further analysis.

TOR is a well-studied pathway in sugar signaling; however, the TOR inhibitor, AZD-8055, did not cancel the inhibitory effect of sucrose on xylem differentiation in VISUAL (Supplementary Fig. S2). It has been reported that sucrose increases the GSK3s-dependent phosphorylation of BRASSINAZOLE RESISTANT 1 (BZR1), the closest homolog of BES1, in the regulation of hypocotyl elongation. However, this effect is considered to be independent of the TOR signaling pathway (Zhang et al. 2021). Recently, it was shown that one of the GSK3s, BRASSINOSTEROID INSENSITIVE2 (BIN2), negatively controls TOR activity to decrease autophagy activity (Liao et al. 2022). Furthermore, reanalysis of transcriptome data revealed that sucrose-responsive gene sets include BIN2 as a downregulated gene and BZR1 as an upregulated gene (Dinant and Le Hir 2022). Although these findings suggest the possible interaction between sucrose signaling and GSK3s–BES/BZR, it remains unknown how a sugar signaling pathway connects with BES/BZR proteins. Further genetic studies, such as a sucrose-insensitive genetic screen using VISUAL, will reveal the molecular mechanisms of sucrose sensing and signaling in the regulation of plant growth and development.

Materials and Methods

Plant materials

All *Arabidopsis* seeds used in this study were from the Col-0 background. To construct the plasmid for estradiol-inducible *CINV1*, the coding sequence of CINV1 without a stop codon was amplified using primers 5′-CACCATGGAAGGTGTTGGACTAAGAGCT-3′ (forward primer) and 5′-GAGTTGTGGCCAAGACGCA-3′ (reverse primer). The amplified sequence was cloned into pENTR/D-TOPO (Thermo Fisher Scientific, Waltham, Massachusetts, USA) and then inserted into the *pER8-GW-CFP* vector via the LR reaction (Thermo Fisher Scientific, Waltham, Massachusetts, USA). The *pER8:CINV1-CFP* plasmid was transformed into the WT using *Agrobacterium tumefaciens* strain GV3101. T3 homozygous lines were used for the analyses. *pIRX3:ELUC* (Kondo 2022) and *gRABC2A-GFP* (Nurani et al. 2020) markers have been reported previously.

VISUAL assay

For VISUAL, *Arabidopsis* seeds were germinated in the half-strength Murashige and Skoog (MS) liquid medium and then grown for 6 d under continuous light (45–55 μmol m^{-2} s^{-1}) at 22°C. The shoots of 6-day-old seedlings were cultured under continuous light (60–70 μmol m^{-2} s^{-1}) at 22°C with the liquid induction medium containing 0.25 mg l^{-1} of 2,4-dichlorophenoxyacetic acid (2,4-D), 1.25 mg l^{-1} kinetin, 20 μM bikinin and 5% (w/v) glucose. To examine the effects of sugars, different types of sugars were used instead of glucose at appropriate concentrations. To visualize the ectopic xylem cells in VISUAL, BF-170 (Sigma-Aldrich, St. Louis, Missouri, USA) was added to the induction medium as a fluorescent indicator of the xylem secondary cell wall (Nurani et al. 2020). As the TOR inhibitor, AZD-8055 (Funakoshi, Tokyo, Japan) was added to the VISUAL induction medium. The xylem differentiation rate (%) was calculated from fluorescence images as the ratio of 'ectopic xylem area' to 'whole leaf area' using ImageJ (Furuya et al. 2021). *pIRX3:ELUC* luminescence was measured with adding 200 μM D-luciferin (FUJIFILM Wako, Osaka, Japan) substrate to white 24-well plates (PerkinElmer, Waltham, Massachusetts, USA). Luminescence was automatically measured approximately every 20 min as photon counts per second using a TriStar2 LB942 luminometer (Berthold Technologies, Bad Wildbad, Germany), which was placed in a growth chamber (Nihonika, Osaka, Japan) with a light-emitting diode illuminator (22°C, 60–70 μmol m^{-2} s^{-1}) (Tamaki et al. 2020).

RT-qPCR

Total RNA was extracted from *pER8:CINV1-CFP* seedlings treated or not treated with 10 μM estradiol for 4 d using the RNeasy Plant Mini Kit (Qiagen, Hilden, Germany). After reverse transcription, qPCR was performed using SYBR Green and was analyzed with a LightCycler (Roche Diagnostics, Basel, Switzerland). Expression levels of *CINV1* (forward primer, 5′-ATGGAAGGT GTTGGACTAAGA-3′; reverse primer, 5′-AGAGTACCAACAGGTTGACC-3′) were normalized using an internal control, *UBQ14* (forward primer, 5′-CAA ATCTCTCAATCGGGATCA-3′; reverse primer, 5′-ACCCTCCTTGTCTTGGATC TT-3′).

Transcriptome analysis

Cotyledons cultured with the VISUAL medium containing 5% (w/v) glucose or 5% (w/v) sucrose were sampled, and then total RNA was extracted using the RNeasy Plant Mini Kit (Qiagen, Hilden, Germany). For microarray analysis, gene expression profiles were comprehensively analyzed with the Arabidopsis ATH1 Genome Array (Affymetrix) according to the previously published method (Ohashi-Ito et al. 2010). RNA-seq analysis was performed using Illumina NovaSeq 6000 (150PE, 4Gb; Rhelixa Co., Ltd, Tokyo, Japan). Obtained raw sequencing data were analyzed with CLC genomics workbench (Qiagen, Hilden, Germany) to calculate transcripts per million (TPM) for each gene. After extracting cambium-, xylem- and phloem-related genes according to the previous gene clustering by Furuya et al. (2021), gene expression values were normalized with *z*-scores. To visualize the similarities of expression profiles of vascular-related genes among the samples, PCA was performed using calculated *z*-scores of gene expression and its result was shown as a three-dimensional plot. For heatmap construction, cambium-, xylem- and phloem-related genes were separately normalized and *z*-scores were shown according to the color scale.

Cross-sections

Arabidopsis seedlings harboring *pER8:CINV1-CFP* were grown in the half-strength MS liquid medium containing 1% (w/v) sucrose for 7 d under continuous light (45–55 μmol m^{-2} s^{-1}), and then DMSO or 10 μM estradiol was added into the medium for a further 4 d. The excised hypocotyls were fixed with formaldehyde-alcohol-acetic acid and ethanol and were then embedded using Technovit 7100 (Kulzer,Hanau, Germany) according to a protocol published previously (Kondo et al. 2014). A RM2165 microtome (Leica, Wetzlar, Germany)

was used to cut the embedded samples into 5-μm-thick sections, which were then examined under a microscope after staining with 0.1% toluidine blue. The minimum number of cambium layers between differentiated xylem and phloem cells was counted according to a previously published protocol (Furuya et al. 2021).

Supplementary Data

Supplementary data are available at *PCP* online.

Data Availability

The microarray data underlying this article are available in Gene Expression Omnibus at https://www.ncbi.nlm.nih.gov/geo/ and can be accessed with the accession number: GSE223284. The sequence reads for RNA-seq were deposited in the DDBJ and are available through the Sequence Read Archive under the accession number DRA015900.

Author Contributions

Y.K. designed the research. A.N. performed VISUAL experiments. A.N., S.S., T.F. and Y.K. performed transcriptome and bioinformatic analyses. A.N., P.K., S.M. and C.O. performed experiments related to sugar. K.I., H.F., C.O. and Y.K. discussed the research. Y.K. wrote the manuscript.

Disclosures

The authors have no conflicts of interest to declare.

References

Aubry, E., Hoffmann, B., Vilaine, F., Gilard, F., Klemens, P.A.W., Guérard, F., et al. (2022) A vacuolar hexose transport is required for xylem development in the inflorescence stem. *Plant Physiol.* 188: 1229–1247.

Chresta, C.M., Davies, B.R., Hickson, I., Harding, T., Cosulich, S., Critchlow, S.E., et al. (2010) AZD8055 is a potent, selective, and orally bioavailable ATP-competitive mammalian target of rapamycin kinase inhibitor with in vitro and in vivo antitumor activity. *Cancer Res.* 70: 288–298.

Damari-Weissler, H., Rachamilevitch, S., Aloni, R., German, M.A., Cohen, S., Zwieniecki, M.A., et al. (2009) LeFRK2 is required for phloem and xylem differentiation and the transport of both sugar and water. *Planta* 230: 795–805.

Dinant, S. and Le Hir, R. (2022) Delving deeper into the link between sugar transport, sugar signaling, and vascular system development. *Physiol. Plant* 174: e13684.

Dong, Y., Uslu, V.V., Berr, A., Singh, G., Papdi, C., Steffens, V.A., et al. (2023) TOR represses stress responses through global regulation of H3K27 trimethylation in plants. *J. Exp. Bot.* 74: 1420–1431. (Online ahead of print).

Dong, P., Xiong, F., Que, Y., Wang, K., Yu, L., Li, Z., et al. (2015) Expression profiling and functional analysis reveals that TOR is a key player in regulating photosynthesis and phytohormone signaling pathways in Arabidopsis. *Front. Plant Sci.* 6: 677.

Etchells, J.P., Smit, M.E., Gaudinier, A., Williams, C.J. and Brady, S.M. (2016) A brief history of the TDIF-PXY signalling module: balancing meristem identity and differentiation during vascular development. *New Phytol.* 209: 474–484.

Etchells, J.P. and Turner, S.R. (2010) The PXY-CLE41 receptor ligand pair defines a multifunctional pathway that controls the rate and orientation of vascular cell division. *Development* 137: 767–774.

Fink, D., Dobbelstein, E., Barbian, A. and Lohaus, G. (2018) Ratio of sugar concentrations in the phloem sap and the cytosol of mesophyll cells in different tree species as an indicator of the phloem loading mechanism. *Planta* 248: 661–673.

Fisher, K. and Turner, S. (2007) PXY, a receptor-like kinase essential for maintaining polarity during plant vascular-tissue development. *Curr. Biol.* 17: 1061–1066.

Fukuda, H. and Hardtke, C.S. (2020) Peptide signaling pathways in vascular differentiation. *Plant Physiol.* 182: 636–1644.

Fu, L., Liu, Y., Qin, G., Wu, P., Zi, H., Xu, Z., et al. (2021) The TOR-EIN2 axis mediates nuclear signalling to modulate plant growth. *Nature* 591: 288–292.

Furuya, T., Saito, M., Uchimura, H., Satake, A., Nosaki, S., Miyakawa, T., et al. (2021) Gene co-expression network analysis identifies BEH3 as a stabilizer of secondary vascular development in Arabidopsis. *Plant Cell* 33: 2618–2636.

Hirakawa, Y., Kondo, Y. and Fukuda, H. (2010) TDIF peptide signaling regulates vascular stem cell proliferation via the WOX4 homeobox gene in Arabidopsis. *Plant Cell* 22: 2618–2629.

Hirakawa, Y., Shinohara, H., Kondo, Y., Inoue, A., Nakanomyo, I., Ogawa, M., et al. (2008) Non-cell-autonomous control of vascular stem cell fate by a CLE peptide/receptor system. *Proc. Natl. Acad. Sci. U.S.A.* 105: 15208–15213.

Hu, J., Hu, X., Yang, Y., He, C., Hu, J. and Wang, X. (2022) Strigolactone signaling regulates cambial activity through repression of WOX4 by transcription factor BES1. *Plant Physiol.* 188: 255–267.

Ito, Y., Nakanomyo, I., Motose, H., Iwamoto, K., Sawa, S., Dohmae, N., et al. (2006) Dodeca-CLE peptides as suppressors of plant stem cell differentiation. *Science* 313: 842–845.

Kondo, Y. (2022) Competitive action between brassinosteroid and tracheary element differentiation inhibitory factor in controlling xylem cell differentiation. *Plant Biotechnol.* 39: 59–64.

Kondo, Y., Fujita, T., Sugiyama, M. and Fukuda, H. (2015) A novel system for xylem cell differentiation in Arabidopsis thaliana. *Mol. Plant* 8: 612–621.

Kondo, Y. and Fukuda, H. (2015) The TDIF signaling network. *Curr. Opin. Plant Biol.* 28: 106–110.

Kondo, Y., Ito, T., Nakagami, H., Hirakawa, Y., Saito, M., Tamaki, T., et al. (2014) Plant GSK3 proteins regulate xylem cell differentiation downstream of TDIF–TDR signalling. *Nat. Commun.* 5: 1–11.

Kondo, Y., Nurani, A.M., Saito, C., Ichihashi, Y., Saito, M., Yamazaki, K., et al. (2016) Vascular Cell Induction Culture System Using Arabidopsis Leaves (VISUAL) reveals the sequential differentiation of sieve element-like cells. *Plant Cell* 28: 1250–1262.

Lemoine, R., La Camera, S., Atanassova, R., Dédaldéchamp, F., Allario, T., Pourtau, N., et al. (2013) Source-to-sink transport of sugar and regulation by environmental factors. *Front. Plant Sci.* 4: 272.

Liao, C.Y., Pu, Y., Nolan, T.M., Montes, C., Guo, H., Walley, J.W., et al. (2022) Brassinosteroids modulate autophagy through phosphorylation of RAPTOR1B by the GSK3-like kinase BIN2 in Arabidopsis. *Autophagy* 24: 1–18.

Li, L. and Sheen, J. (2016) Dynamic and diverse sugar signaling. *Curr. Opin. Plant Biol.* 33: 116–125.

Lou, Y., Gou, J.Y. and Xue, H.W. (2007) PIP5K9, an Arabidopsis phosphatidylinositol monophosphate kinase, interacts with a cytosolic invertase to negatively regulate sugar-mediated root growth. *Plant Cell* 19: 163–181.

Lugassi, N., Stein, O., Egbaria, A., Belausov, E., Zemach, H., Arad, T., et al. (2022) Sucrose synthase and fructokinase are required for proper meristematic and vascular development. *Plants* 11: 1035.

Moore, B., Zhou, L., Rolland, F., Hall, Q., Cheng, W.H., Liu, Y.X., et al. (2003) Role of the Arabidopsis glucose sensor HXK1 in nutrient, light, and hormonal signaling. *Science* 300: 332–336.

Nurani, A.M., Ozawa, Y., Furuya, T., Sakamoto, Y., Ebine, K., Matsunaga, S., et al. (2020) Deep imaging analysis in VISUAL reveals the role of YABBY genes in vascular stem cell fate determination. *Plant Cell Physiol.* 61: 255–264.

Ohashi-Ito, K., Oda, Y. and Fukuda, H. (2010) Arabidopsis VASCULAR-RELATED NAC-DOMAIN6 directly regulates the genes that govern programmed cell death and secondary wall formation during xylem differentiation. *Plant Cell* 22: 3461–3473.

Saito, M., Kondo, Y. and Fukuda, H. (2018) BES1 and BZR1 redundantly promote phloem and xylem differentiation. *Plant Cell Physiol.* 59: 590–600.

Shimadzu, S., Furuya, T. and Kondo, Y. (2023) Molecular mechanisms underlying the establishment and maintenance of vascular stem cells in Arabidopsis thaliana. *Plant Cell Physiol.* 64: 274–283. Online ahead of print.

Shi, D., Tavhelidse, T., Thumberger, T., Wittbrodt, J. and Greb, T. (2017) Bifacial stem cell niches in fish and plants. *Curr. Opin. Genet. Dev.* 45: 28–33.

Shi, L., We, Y. and Sheen, J. (2018) TOR signaling in plants: conservation and innovation. *Development* 145: dev160887.

Subramanian, A., Tamayo, P., Mootha, V.K., Mukherjee, S., Ebert, B.L., Gillette, M.A., et al. (2005) Gene set enrichment analysis: a knowledge-based approach for interpreting genome-wide expression profiles. *Proc. Natl. Acad. Sci. U.S.A.* 102: 15545–15550.

Tamaki, T., Oya, S., Naito, M., Ozawa, Y., Furuya, T., Saito, M., et al. (2020) VISUAL-CC system uncovers the role of GSK3 as an orchestrator of vascular cell type ratio in plants. *Commun. Biol.* 3: 184.

Uggla, C., Magel, E., Moritz, T. and Sundberg, B. (2001) Function and dynamics of auxin and carbohydrates during earlywood/latewood transition in Scots pine. *Plant Physiol.* 125: 2029–2039.

Xiang, L., Le Roy, K., Bolouri-Moghaddam, M.R., Vanhaecke, M., Lammens, W., Rolland, F., et al. (2011) Exploring the neutral invertase-oxidative stress defence connection in Arabidopsis thaliana. *J. Exp. Bot.* 62: 3849–3862.

Ye, R., Wang, M.H., Du, H. Chhajed, S., Koh, J., Liu, K.H., et al. (2022) Glucose-driven TOR-FIE-PRC2 signalling controls plant development. *Nature* 609: 986–993.

Yin, Y., Wang, Z.Y., Mora-Garcia, S., Li, J., Yoshida, S., Asami, T., et al. (2002) BES1 accumulates in the nucleus in response to brassinosteroids to regulate gene expression and promote stem elongation. *Cell* 109: 181–191.

Zhang, Z., Sun, Y., Jiang, X., Wang, W. and Wang, Z.Y. (2021) Sugar inhibits brassinosteroid signaling by enhancing BIN2 phosphorylation of BZR1. *PLoS Genet.* 17: e1009540.